Ultrafast dynamics of autoionizing states in O_2 probed by laser-field-assisted XUV photoionization

Changjun Zhu,[1,2] Dong Hyuk Ko,[1,3] Kyung Sik Kang,[1,3] Jisu Lee,[1,3] Jae-hwan Lee,[3] G. Umesh,[4] E. Krishnakumar,[5] and Chang Hee Nam[1,3,*]

[1]*Department of Physics, KAIST, Daejeon 305-701, Korea*

[2]*Department of Physics, School of Science, Xi'an Polytechnic University, Xi'an 710048, China*

[3]*Center for Relativistic Laser Science, Institute for Basic Science (IBS), Gwangju 500-712, Korea*

[4]*Physics Department, National Institute of Technology Karnataka, Surathkal, Mangalore 575025, India*

[5]*Tata Institute of Fundamental Research, Homi Bhabha Road, Mumbai 400005, India*

(Received 6 November 2012; revised manuscript received 19 May 2013; published 16 October 2013)

Dynamics of the autoionizing states in O_2 was investigated using the method of laser-field-assisted extreme-ultraviolet photoionization. Harmonics, ranging from 9th to 21st orders generated in Kr with 25 fs laser pulses at 820 nm, were employed to carry out photoionization of O_2. Distinct autoionization features in the photoelectron spectrum, stemming from the resonant excitation of superexcited states of O_2 by the 11th harmonic, were observed. The superexcited states, referred to as autoionizing states, were identified to be the $\nu' = 0$, $n = 5$ Rydberg states converging to the $b\,^4\Sigma_g{}^-$ state of $O_2{}^+$. Infrared laser pulses were utilized as the probe to monitor time-varying characteristics of photoionization and autoionization of O_2. A decay time of 21 fs was obtained for the autoionizing states of O_2 by deconvoluting the pump-probe results in O_2 and Ar.

DOI: 10.1103/PhysRevA.88.043419 PACS number(s): 33.80.Eh, 33.60.+q, 33.20.Xx, 33.80.Rv

I. INTRODUCTION

Photoionization has been extensively investigated in atoms and molecules as the photoelectron spectra can provide abundant information on the energy level structure of atoms and molecules. Photoionization wherein electrons are directly ionized in a very short time is not a resonant process, and the excess photon energy appears as kinetic energy of the photoelectrons. In contrast, autoionization is an indirect ionization process that occurs after a resonant excitation. In this case atoms and molecules are first resonantly excited to superexcited states, i.e., excited neutral states with energy above the first ionization potential, and they then release electrons spontaneously. If the photon energies lie above the first ionization potential, and fall into resonant excitation regions, autoionization occurs concurrently in a photoionization process and interferes with the direct photoionization process, leading to variations in the photoelectron spectrum. Specifically, in molecular photoelectron spectra, autoionization alters the vibrational structure of electron bands and changes the relative band intensities.

Much attention has hitherto been focused on the investigations of photoionization of O_2. Experiments have been conducted using the He I line radiation at 58.4 nm [1] and synchrotron radiation [2] as light sources. Meanwhile, considerable effort has been devoted to the study of autoionization in O_2 with photons of various energies [3]. Photoionization of oxygen molecules by high-order harmonics was investigated and the photoelectron spectrum not only exhibited multiple peaks resulting from different orders of harmonics, but also displayed a clean contribution from autoionizing states which were resonantly excited by the 11th harmonic [4]. These studies have greatly enriched our knowledge of photoionization and autoionization, in terms of absorption coefficients, ionization cross section, and competing mechanisms. Nevertheless, all the aforementioned investigations revealed only the static aspects of the photoionization and autoionization since only time-integrated photoelectron spectra of O_2 were studied.

Recently, remarkably rapid advances in ultrafast light sources, especially the advent of attosecond pulse trains [5,6] and single attosecond pulses [7,8], have opened up a route to time-resolved investigation of ultrafast phenomena with attosecond temporal resolution. For instance, time-resolved inner shell atomic spectroscopy [9] and attosecond atomic electron wave packet dynamics [10] have been examined recently by time-resolved pump-probe experiments using attosecond pulses obtained via high harmonic generation. More interestingly, investigations on ultrafast molecular dynamics have been initiated [11,12]. With a view to carrying out time-resolved studies on autoionization, most investigations were devoted to atomic systems [13,14], and very little effort has been devoted to examining ultrafast dynamics relating to the evolution of autoionizing states in molecules [15,16]. Recently, the phase of the two-color two-photon ionization transition (molecular phase) for different states of the ion was measured [17]. Furthermore, ultrafast decay of superexcited $c^4\Sigma_u - n^1\sigma_g\nu = 0,1$ states of O_2 was investigated with femtosecond photoelectron spectroscopy [18]. The study of molecular autoionization, associated with molecular Rydberg wave packets, has become a rapidly expanding topic. Direct observation of the dynamics of autoionizing states in molecules is of fundamental significance in exploring the underlying mechanisms governing the formation of photoelectron spectra produced in molecular ionization processes and, in particular, in unveiling the intriguing characteristics of evolution and decay of molecular autoionizing states. We present in this paper a time-resolved investigation into the decay dynamics of autoionizing states in O_2 by laser-field-assisted extreme-ultraviolet (XUV) photoionization.

*Present address: Department of Physics and Photon Science, Gwangju Institute of Science and Technology, Gwangju 500-712, Korea.

 ©2013 American Physical Society

II. EXPERIMENT SETUP

Experiments were conducted with a setup similar to the one shown in Ref. [19]. Briefly, linearly polarized laser pulses, with energy of 1.5 mJ, were generated from a femtosecond Ti:sapphire laser at a repetition rate of 1 kHz. The wavelength of the laser was centered at 820 nm and the pulse duration was 25 fs. The laser pulse was split into two by a beam splitter with 80% transmission. One beam, referred to as pump beam, was blocked by a 2-mm-diameter mask at the beam center to form a beam with annular cross section, and then focused into Kr gas in a cell to generate high harmonics leading to formation of XUV pulses. After the harmonic generation the pump IR beam was blocked using an aperture in order to transmit only the harmonics. The other beam, referred to as probe, propagated through an optical delay line and recombined with the XUV beam. This femtosecond infrared (IR) probe laser pulse was delayed with respect to the XUV pulse using a time delay stage. The polarizations of the two beams were parallel. After recombination, the two beams propagated collinearly and were refocused by an Au-coated toroidal mirror onto an effusive molecular beam of O_2. Photoelectrons resulting from the photoionization of the molecular beam were detected using a time-of-flight electron spectrometer equipped with a microchannel plate as the detector. Photoelectron spectra were thus collected for different time delays.

III. RESULTS AND DISCUSSIONS

Figure 1(a) shows the schematic energy level diagram of O_2 relating to the photoionization (blue arrows) and autoionization (red arrows). Figure 1(b) shows the generation of photoelectrons by laser-field-assisted XUV photoionization and autoionization, with the right blue arrow and the left blue arrow representing photoionization and autoionization by the 11th harmonic, respectively. A photoelectron spectrum of O_2 produced by a group of harmonics in our experiments, as shown in Fig. 2(a), exhibits distinct features compared to that created by the He I line. The photoelectron spectrum produced by the He I line exhibits quite a good spectral resolution due to the extremely narrow width of the He I line, displaying five distinct vibrational peak structures representing the formation of vibrational states in the electronic bands $X\,^2\Pi_g$ of $O_2{}^+$ by direct photoionization [1] and, moreover, the photoelectron spectrum contains mainly five electronic bands corresponding to the formation of the first five electronic states of $O_2{}^+$, with two electronic bands, $a\,^4\Pi_u$ and $A\,^2\Pi_u$, seen to be merged [20]. In contrast, one distinct feature of the photoelectron spectra obtained in our experiments is that, in the first electronic band $X\,^2\Pi_g$ of $O_2{}^+$, more than five vibrational peaks were generated by the 11th harmonic. Vibrational peaks corresponding to $v = 0{-}4$ in the ground electronic state $X\,^2\Pi_g$ of $O_2{}^+$ were largely produced by photoionization, whereas vibrational peaks corresponding to $v = 5{-}11$ in the ground electronic state $X\,^2\Pi_g$ of $O_2{}^+$ were predominantly produced by autoionization [4,21], as shown in the inset of Fig. 2(a). The photon energy of the 11th harmonic was 16.6 eV with a bandwidth of 0.15 eV, which is sufficient to resonantly excite the $v' = 0, n = 5$ Rydberg states of O_2 converging to the $b\,^4\Sigma_g{}^-$ state of $O_2{}^+$ [22], suggesting that the superexcited states, i.e., the autoionizing states, are the $v' = 0, n = 5$ Rydberg states.

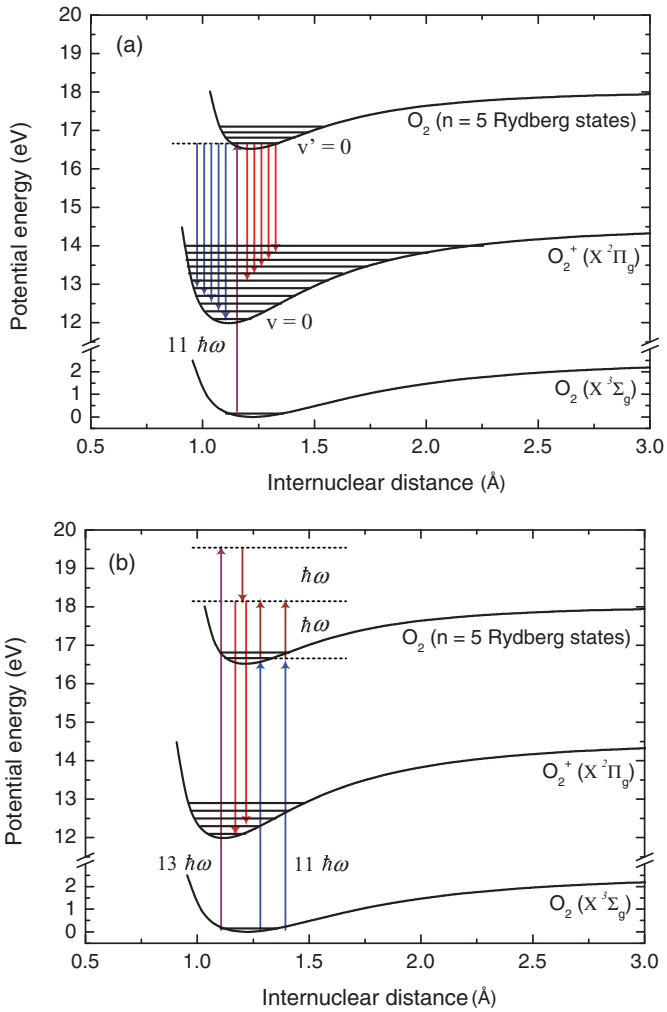

FIG. 1. (Color online) (a) Photoionization and autoionization in O_2 produced by the 11th harmonic. (b) Photoelectron generation in O_2 through sideband 12 by the direct photoionization and autoionization by the 11th harmonic and the direct ionization by the 13th harmonic coupled with the IR probe laser pulse.

Of particular interest is the investigation of the decay of autoionizing states, which reveals the transient characteristics of related electronic and vibrational energy levels of O_2. To gain insight into the autoionization dynamics, a pump-probe scheme was implemented to record time-resolved photoelectron spectra. The wavelength of the laser was centered at 820 nm, corresponding to a photon energy of 1.51 eV. The ionization potential of the first vibrational states in the electronic state $X\,^2\Pi_g$ of $O_2{}^+$ is 12.1 eV. In the pump-probe scheme, XUV pulses served as the pump and IR laser pulses as the probe. The IR probe pulses had a twofold influence on the XUV pulse-induced photoionization. On the one hand, as the molecule is excited by the 11th harmonic into the autoionizing states, the IR pulses perform a sequential ionization, thereby opening the way for observing the decay of autoionizing states by depopulating them. Secondly, the IR field interferes with the XUV field, modulating the time-varying characteristics of the photoelectron spectrum with the time delay scan.

The time-varying photoelectron spectrum exhibits interesting characteristics. Depending on the origin, the photoelectron

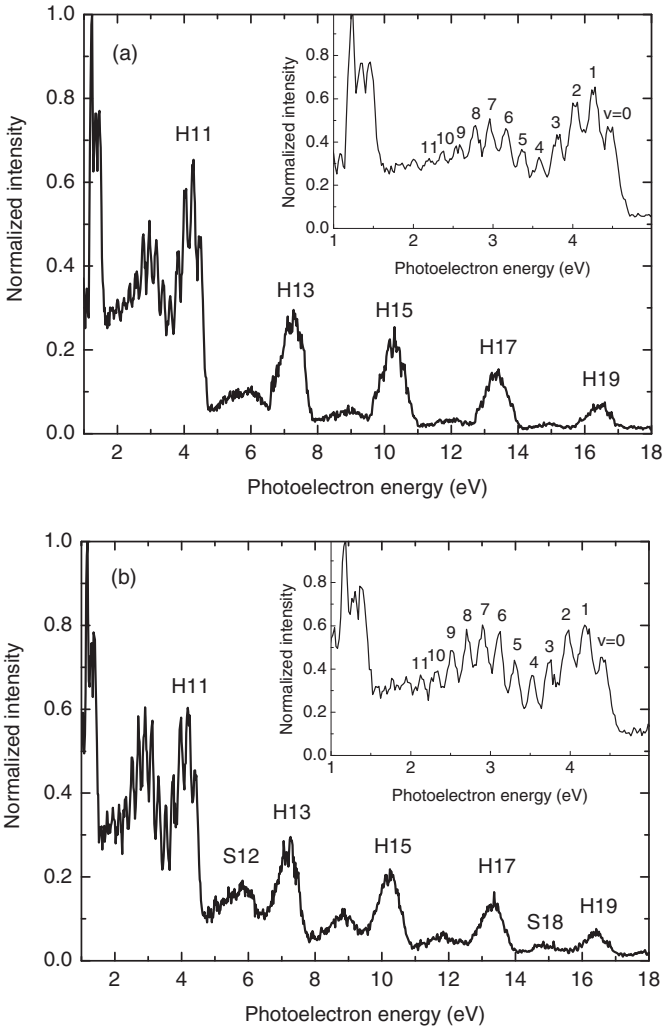

FIG. 2. (a) Photoelectron spectra in O_2 recorded only with high harmonics. (b) Photoelectron spectra in O_2 recorded with high harmonics and IR. The insets display the vibrational photoelectron peaks produced by the 11th harmonic through direct photoionization ($v = 0$–4) and autoionization ($v = 5$–11) on expanded scales.

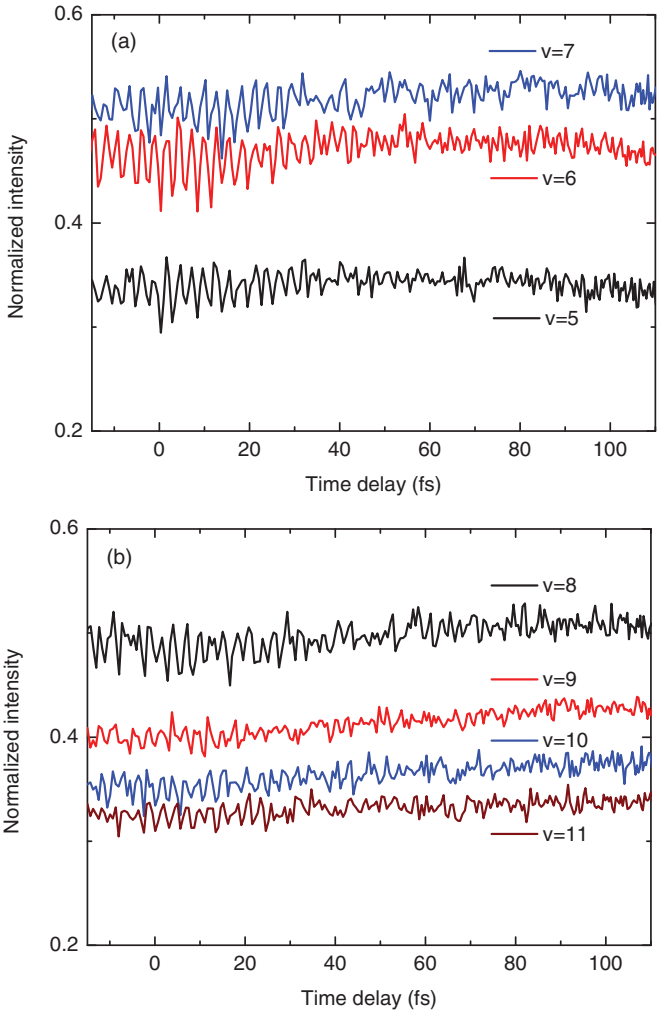

FIG. 3. (Color online) Time-varying characteristics of vibrational photoelectron peaks, (a) $v = 5$–7 and (b) $v = 8$–11, produced in O_2 through autoionization by the 11th harmonic.

peaks in the experimentally acquired photoelectron spectrum can be divided into three categories. As shown in Fig. 2(b), the first category of photoelectron peaks, located at 4.3, 7.3, 10.3, 13.4, and 16.4 eV, are produced due to the direct photoionization by the 11th, 13th, 15th, 17th, and 19th harmonics, respectively. The second category of photoelectron peaks, situated at 5.8, 8.8, 11.8, and 14.9 eV, are the 12th, 14th, 16th, and 18th sidebands, respectively. These sidebands originate from the interference between two processes, namely, the absorption of an XUV photon and an IR photon, and the absorption of an XUV photon and emission of an IR photon. They are generated only when the XUV pulse overlaps spatially and temporally with the IR pulse in O_2. The third category of photoelectron peaks corresponding to $v = 5-11$ in the ground electronic state $X\,^2\Pi_g$ of O_2^+, ranging from 2.1 to 3.3 eV, with approximate energy intervals of 0.2 eV, is produced due to autoionization by the 11th harmonic, as shown in the inset of Fig. 2(b). They are formed by the process wherein O_2 is resonantly excited to the superexcited $\nu' = 0$, $n = 5$ Rydberg states and then autoionizes, forming vibrational states in the electronic state $X\,^2\Pi_g$ of O_2^+.

Difficulties in analyzing the decay of autoionizing states arise as one tries to acquire the decay dynamics of the autoionizing states by directly observing the time-varying characteristics of photoelectron peaks ($v = 5-11$) ranging from 2.1 to 3.3 eV, which are closely related to the decay of the autoionizing states. The time-varying characteristics of the photoelectron peaks ranging from 2.1 to 3.3 eV exhibit complicated features rather than a monotonic decay owing to the overlap in energy with the 10th sideband produced by the interaction of the 9th and 11th harmonics with the IR probe pulses, as shown in Fig. 3.

The aforementioned difficulties can be overcome by comparing the time-varying characteristics of sideband 12 in O_2 with that of sideband 12 produced in Ar. It should be noted that the signal obtained in O_2 consists of photoelectrons generated from both direct ionization and autoionization. Specifically, there are two sources of photoelectrons for the sideband 12 in O_2, as shown in Fig. 1(b). The first comes from the direct ionization by the process $[(11 + 1)h\nu + (13 - 1)h\nu]$. The second is from the process of pump $(11h\nu)$ + probe $(h\nu)$,

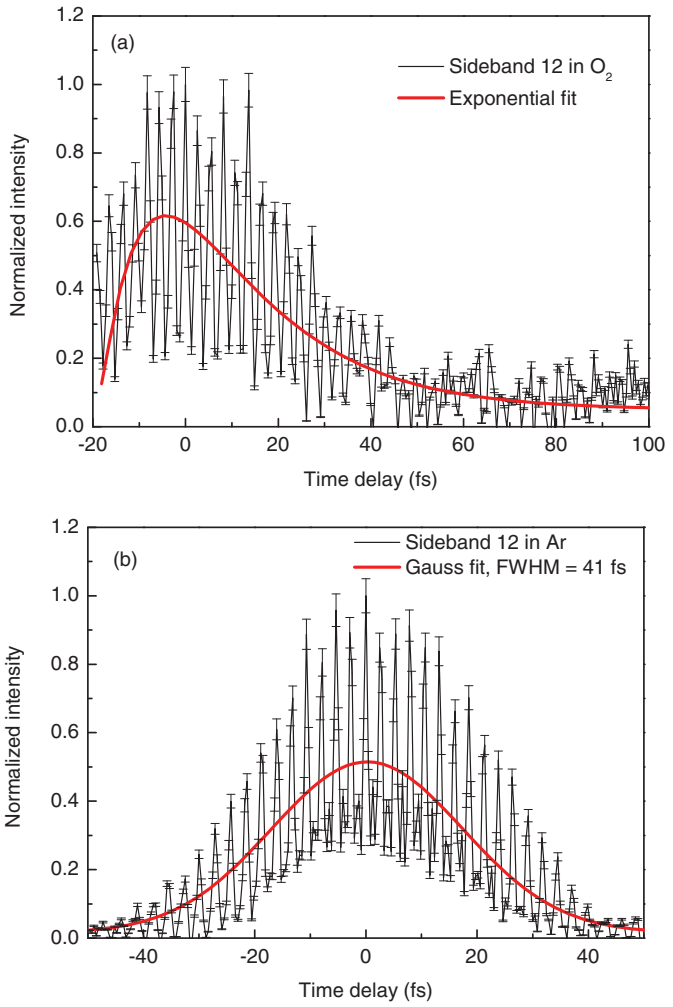

FIG. 4. (Color online) Time-varying characteristics of photoelectrons for (a) sideband 12 in O_2 and (b) sideband 12 in Ar (black: experimental data; red: fittings).

in which the molecule is first excited by the XUV pulses into the autoionizing states and then sequentially ionized further by the IR. Thus, for the sideband 12 in O_2, photoelectrons released by the autoionization through pump $(11h\nu)$ + probe $(h\nu)$, are mixed with the photoelectrons produced by the direct ionization. On the other hand, for the sideband 12 in Ar, photoelectrons are produced purely by direct photoionization. In other words, the sideband 12 in O_2 contains photoelectrons produced through photoionization and autoionization of O_2 by the 11th harmonic, whereas the sideband 12 in Ar merely contains photoelectrons released from the direct photoionization of Ar by the interaction of IR with 11th and 13th harmonics. The two kinds of photoelectrons, produced in O_2 by the direct photoionization and the autoionization process, respectively, emerge at different times, suggesting that the time-varying characteristics of sideband 12 in O_2 are different from that of sideband 12 in Ar. This point was clearly proved in our experimental results, as shown in Fig. 4.

Further insight into the decay of autoionizing states can be obtained by examining the time-varying characteristics of the sidebands 12 in O_2 and sideband 12 in Ar. The sideband 12 in O_2 can be expressed by the convolution among XUV pulses,

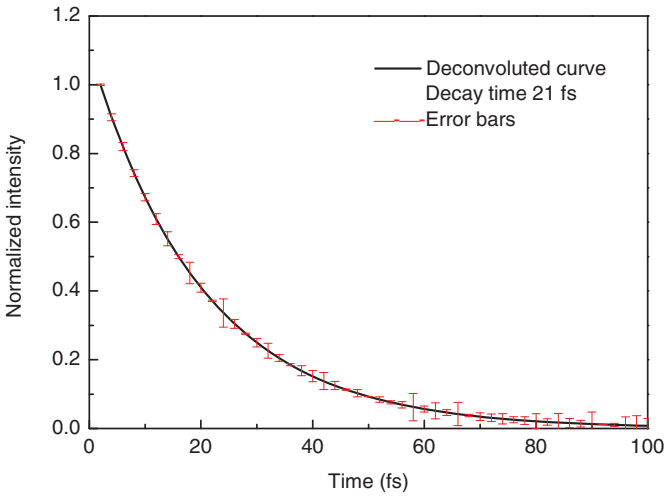

FIG. 5. (Color online) Deconvolution result of sideband 12 in O_2 and sideband 12 in Ar.

IR pulses, and decay of autoionizing states

$$S_{12} = \mathrm{XUV} * \mathrm{IR} * \mathrm{D}, \tag{1}$$

where D represents decay and $*$ denotes convolution. Since the sideband 12 in Ar is generated by the interaction of IR with 11th and 13th harmonics through direct ionization, it can be expressed as

$$S'_{12} = \mathrm{XUV} * \mathrm{IR}. \tag{2}$$

The decay of autoionization can thus be extracted by deconvoluting the sideband 12 in Ar out of the sideband 12 in O_2. Toward this end, double exponential fitting and Gaussian fitting were made for the sideband 12 in O_2 and the sideband 12 in Ar, respectively, as shown in Fig. 4. The double exponential fitting for the sidebands 12 in O_2 is expressed as

$$y = 0.052\,23 + 0.735\,\exp\left[-\left(\frac{x-5.929}{19.652}\right)\right] - 0.259\,\exp\left[-\left(\frac{x-5.929}{10.671}\right)\right]. \tag{3}$$

The Gauss fitting for the sidebands 12 in Ar is expressed as

$$y = 0.0164 + \frac{21.502}{34.441\sqrt{\frac{\pi}{2}}}\exp\left[-2\left(\frac{x-1.229}{34.441}\right)^2\right]. \tag{4}$$

Deconvoluting Eq. (4) out of Eq. (3) yields a single exponential curve with a decay time of 21 fs, as shown in Fig. 5, corresponding to the lifetime of the autoionizing states. Since the autoionizing states can decay to different vibrational states of $X\,^2\Pi_g$ in $O_2{}^+$, the lifetime of the autoionizing states is an average value.

The time-resolved photoelectron spectra in O_2, obtained by using the XUV + IR scheme, reveal interesting time-varying modulation characteristics of photoelectron peaks. Modulation of sidebands at half optical cycle was exploited previously in atoms to characterize attosecond pulses in the reconstruction of attosecond beating by interference of two-photon transition (RABITT) measurement [4,5]. In our current experiments, nevertheless, a modulation period of one optical cycle (2.7 fs) for the photoelectron peaks and sidebands, rather than a half

optical cycle, was displayed, as shown in Figs. 3 and 4. Specifically, the photoelectron peaks and sidebands modulate with the time delay between XUV and IR pulses at a rate equal to the IR frequency. The one cycle modulation in the photoelectron peaks and sidebands might be attributed to the leakage of the pump IR beam after the harmonic generation. As the time delay between XUV and IR is changed, the leaked IR pulses interfere with the probe IR pulses, changing the balance in IR intensity during one optical cycle due to the constructive and destructive interference between the probe and the leaked pulses. Since the leaked IR was minimal because of careful optical alignment, the effect on the decay time would not be serious. The modulation period of photoelectron peaks and sidebands needs to be explored further in order to clarify the excitation and ionization processes in molecules and to investigate a potential route to dynamic control of molecular ionization.

IV. CONCLUSION

The evolution and decay dynamics of the autoionizing states in O_2 was investigated by employing laser-field-assisted XUV photoionization, in which the IR laser pulses were utilized as the probe to monitor time-varying characteristics of photoionization and autoionization of O_2. Remarkable autoionization features showed up in the photoelectron spectrum and the autoionizing states were identified to be the $v' = 0$, $n = 5$ Rydberg states of O_2 converging to the $b\ ^4\Sigma_g^-$ state of O_2^+. The pump-probe experiments revealed that time-varying characteristics of the sideband 12 in O_2, intimately associated with autoionization, were distinctly different from that of the sideband 12 in Ar, which were closely related to direct photoionization. Deconvolution was implemented to retrieve the decay of autoionizing states and, as a result, a decay time of 21 fs was obtained for the autoionizing states of O_2. Further investigations into photoionization and autoionizing dynamics in O_2 will eventually lead to precise, active control and manipulation of photoionization, autoionization, and dissociation processes of molecules.

ACKNOWLEDGMENT

This research was supported by Institute for Basic Science and by National Research Foundation, Korea.

[1] P. Baltzer, B. Wannberg, L. Karlsson, M. Carlsson Göthe, and M. Larsson, Phys. Rev. A **45**, 4374 (1992).
[2] A. Lafosse, J. C. Brenot, A. V. Golovin, P. M. Guyon, K. Hoejrup, J. C. Houver, M. Lebech, and D. Dowek, J. Chem. Phys. **114**, 6605 (2001).
[3] A. V. Golovin, F. Heiser, C. J. K. Quayle, P. Morin, M. Simon, O. Gessner, P.-M. Guyon, and U. Becker, Phys. Rev. Lett. **79**, 4554 (1997).
[4] K. T. Kim, K. S. Kang, M. N. Park, T. Imran, C. Zhu, C. H. Nam, E. Krishnakumar, and G. Umesh, J. Korean Phys. Soc. **49**, 309 (2006).
[5] Y. Mairesse, A. de Bohan, L. J. Frasinski, H. Merdji, L. C. Dinu, P. Monchicourt, P. Breger, M. Kovacev, R. Taïeb, B. Carré, H. G. Muller, P. Agostini, and P. Salières, Science **302**, 1540 (2003).
[6] D. H. Ko, K. T. Kim, J. Park, J.-h. Lee, and C. H. Nam, New J. Phys. **12**, 063008 (2010).
[7] K. T. Kim, C. M. Kim, M.-G. Baik, G. Umesh, and C. H. Nam, Phys. Rev. A **69**, 051805(R) (2004).
[8] A. Baltuka, Th. Udem, M. Uiberacker, M. Hentschel, E. Goulielmakis, Ch. Gohle, R. Holzwarth, V. S. Yakovlev, A. Scrinzi, T. W. Hänsch, and F. Krausz, Nature (London) **421**, 611 (2003).
[9] M. Drescher, M. Hentschel, R. Kienberger, M. Uiberacker, V. Yakovlev, A. Scrinzi, Th. Westerwalbesloh, U. Kleineberg, U. Heinzmann, and F. Krausz, Nature (London) **419**, 803 (2002).
[10] P. Johnsson, R. López-Martens, S. Kazamias, J. Mauritsson, C. Valentin, T. Remetter, K. Varjú, M. B. Gaarde, Y. Mairesse, H. Wabnitz, P. Salières, Ph. Balcou, K. J. Schafer, and A. L'Huillier, Phys. Rev. Lett. **95**, 013001 (2005).
[11] H. Niikura, F. Légaré, R. Hasbani, M. Y. Ivanov, D. M. Villeneuve, and P. B. Corkum, Nature (London) **421**, 826 (2003).
[12] X. M. Tong, Z. X. Zhao, and C. D. Lin, Phys. Rev. Lett. **91**, 233203 (2003).
[13] S. Cavalieri and R. Eramo, Phys. Rev. A **58**, R4263 (1998).
[14] H. Wang, M. Chini, S. Chen, C.-H. Zhang, Y. Cheng, F. He, Y. Wu, U. Thumm, and Z. Chang, Phys. Rev. Lett. **105**, 143002 (2010).
[15] R. Guillemin, M. Simon, and E. Shigemasa, Phys. Rev. A **82**, 051401(R) (2010).
[16] S. De, I. A. Bocharova, M. Magrakvelidze, D. Ray, W. Cao, B. Bergues, U. Thumm, M. F. Kling, I. V. Litvinyuk, and C. L. Cocke, Phys. Rev. A **82**, 013408 (2010).
[17] S. Haessler, B. Fabre, J. Higuet, J. Caillat, T. Ruchon, P. Breger, B. Carré, E. Constant, A. Maquet, E. Mével, P. Salières, R. Taïeb, and Y. Mairesse, Phys. Rev. A **80**, 011404(R) (2009).
[18] Benjamin Doughty, Christine J. Koh, Louis H. Haber, and Stephen R. Leone, J. Chem. Phys. **136**, 214303 (2012).
[19] K. T. Kim, K. S. Kang, M. N. Park, T. Imran, G. Umesh, and C. H. Nam, Phys. Rev. Lett. **99**, 223904 (2007).
[20] D. W. Turner, C. Baker, A. D. Baker, and C. R. Brundle, *Molecular Photoelectron Spectroscopy* (Wiley - Interscience, London, 1970), p. 36.
[21] D. Cubric, A. A. Willis, J. Comer, and P. Hammond, J. Phys. B **29**, 4151 (1996).
[22] T. A. York and J. Comer, J. Phys. B **15**, 4629 (1982).